

Electrochemical reduction of CO₂ to formate at high current density using gas diffusion electrodes

D. Kopljar · A. Inan · P. Vindayer ·
N. Wagner · E. Klemm

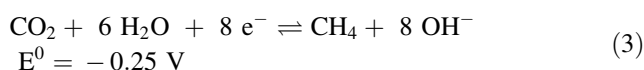
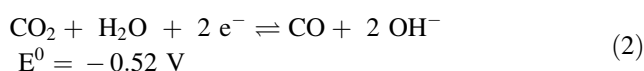
Received: 28 May 2014 / Accepted: 18 August 2014 / Published online: 24 August 2014
© Springer Science+Business Media Dordrecht 2014

Abstract The electrochemical reduction of carbon dioxide into formate was studied using gas diffusion electrodes (GDE) with Sn as electrocatalyst in order to overcome mass transport limitations and to achieve high current densities. For this purpose, a dry pressing method was developed for GDE preparation and optimized with respect to mechanical stability and the performance in the reduction of CO₂. Using this approach, GDEs can be obtained with a high reproducibility in a very simple, fast, and straightforward manner. The influence of the metal loading on current density and product distribution was investigated. Furthermore, the effect of changing the electrolyte pH was evaluated. Under optimized conditions, the GDE allowed current densities up to 200 mA cm⁻² to be achieved with a Faradaic efficiency of around 90 % toward formate and a substantial suppression of hydrogen production (<3 %) at ambient pressure. At higher current densities mass transport issues come into effect and hydrogen is increasingly produced. The corresponding cathode potential was found to be 1.57 V vs. SHE.

Keywords Carbon dioxide · Electrochemical CO₂ reduction · Gas diffusion electrodes · Formate · Formic acid

1 Introduction

In light of the ever-increasing energy demands due to a growing population and a constant rise in living standards around the world, the accumulation of the greenhouse gas CO₂ in the atmosphere constitutes a severe challenge for modern society. Approaches to alleviate emissions are manifold. They range from the employment of clean and more efficient technologies with lower carbon footprint to the development of processes that utilize CO₂ as feedstock. One attractive way for existing plants to reduce their footprint is to capture and process effluent streams rich in CO₂, and to subsequently convert the unwanted greenhouse gas into valuable products [1, 2]. Processes that produce relatively pure CO₂ streams, and are, therefore, particularly qualified are, e.g., the ammonia or ethylene oxide synthesis, biogas purification or certain refinery, and fermentation processes [3]. By means of electrochemical cathodic activation, among other methods, CO₂ can serve as carbon source to produce formic acid, CO or methane according to Eqs. 1–3 (E⁰ vs. SHE at 25 °C and pH 7.0 [4]), while water can serve as a proton and electron donor on the opposing anode side.



Given the finiteness and increasing price of petroleum and natural gas, this is an increasingly attractive route that is currently encouraging a lot of research effort, in both

D. Kopljar (✉) · A. Inan · P. Vindayer · E. Klemm
Institute of Chemical Technology, University of Stuttgart,
Pfaffenwaldring 55, 70569 Stuttgart, Germany
e-mail: dennis.kopljar@itc.uni-stuttgart.de

N. Wagner
German Aerospace Center (DLR), Institute of Engineering
Thermodynamics, Pfaffenwaldring 38-40, 70569 Stuttgart,
Germany

fundamentals and applications [5–11]. In this respect, formic acid is a particularly convenient product, as its current production route is neither straightforward nor environmentally benign, and because it is a suitable hydrogen donor for fuel cells. Thus, its electrochemical production would allow for the storage of electricity in chemical form with formic acid as a non-toxic energy carrier that is easy to store and handle and which can later be decomposed to hydrogen or directly fed into direct-formic acid fuel cells to produce electricity when it is needed [12, 13]. Yet, for this approach to be reasonable, formic acid has to be produced from CO₂ efficiently in the first place. The corresponding reaction has been studied extensively on several electrode materials in order to show its feasibility and to elucidate mechanistic aspects. For formic acid/formate production (at commonly employed pH values, formate is the major product), Sn, Hg, Pb, In, Cd, and Cu have been shown to be favorable electrocatalysts [14, 15]. This is due to their high overpotentials toward the hydrogen evolution reaction (HER, Eq. 4) which, in aqueous electrolytes, occurs within the same potential range and is therefore the main side reaction that decreases selectivity at certain reaction conditions:



Using the above, metals allows for the production of formate with a high Faradaic efficiency (FE, percentage of charge going into the desired product) around 90 % [16]. However, the achievable current density on flat electrodes is limited to approximately 5 mA cm⁻² by the amount of CO₂ that is dissolved in the electrolyte. In contrast, for industrial application high space–time yields are mandatory what requires current densities above 100 mA cm⁻² [7]. Apart from the use of high pressure or organic electrolytes, both of which increase the amount of dissolved CO₂, an approach that has been shown to circumvent solubility limitations is the use of gas diffusion electrodes (GDE), first introduced for this reaction by Mahmood et al. [17]. The porous electrode comprises a high surface area matrix of carbon support and a hydrophobic binding agent into which the catalyst is dispersed. This allows the interfacial area to be formed within the material of the electrode and the three-phase boundary gas/electrolyte/catalyst where the reaction takes place to be massively enhanced. Furthermore, solubility issues are reduced since the gas molecules only have to diffuse through a very thin layer of electrolyte in order to reach the electrode surface. As the effective area is much larger than the geometric area, the observable reaction rates are usually an order of magnitude higher than on conventional flat electrodes. Accordingly, partial current densities up to 130 mA cm⁻² for formate production at ambient pressure have been reported using GDEs [17–19] and even higher values for gaseous products

[20–22]. Besides FE and current density, from an energetic point of view another essential parameter that determines the efficiency of the process is the necessary overpotential to drive the reaction at a given rate. Thus, its minimization is a key challenge that must be approached, e.g., by catalyst optimization and by the minimization of resistances toward mass transport and electron transfer inside the GDE.

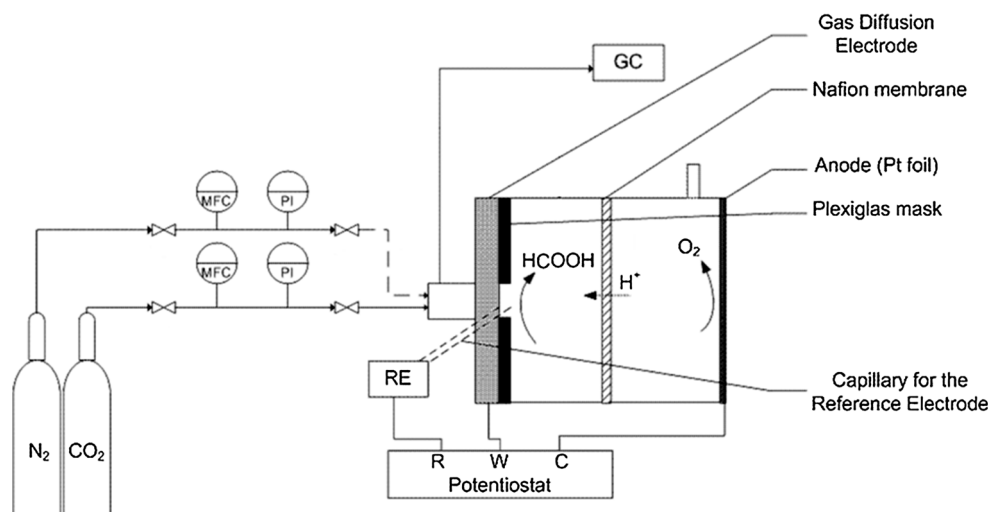
In order to approach this goal, different technologies exist for the GDE preparation which are suitable for industrial production to different degrees. In most of the scientific work published, GDEs are prepared via wet deposition methods in which an ink, usually consisting of a highly concentrated suspension of the catalyst, carbon material and binding agent (mostly PTFE) must be prepared, then sprayed or screen-printed on a support and dried [23]. This is a time-consuming procedure for which scale-up to mass production is suggested to be difficult [24]. In this study, a dry pressing method that greatly simplifies the GDE production procedure is introduced and optimized. The components simply have to be mixed physically, pressed onto a carbon paper support, and sintered. The absence of a solvent, reduction of process steps, and amount of parameters to be optimized make this approach both economically and environmentally sound, and easy to scale-up. Based on this approach, in the framework of this work, the emphasis was put on the feasibility of the electrochemical formate production within an industrial environment. To take this into account, the non-toxic and inexpensive tin was chosen as catalyst and an aqueous solution of KHCO₃ used as electrolyte. At the anode, water electrolysis is responsible for the supply of electrons to the cathode; a previous hydrogen formation step and the handling of molecular hydrogen are thereby omitted. While the overall goal of the project is to incorporate the obtained results into a continuous reactor setup, the reported results herein should act as a starting point to evaluate and optimize the performance and the pressing procedure of the GDE in order to demonstrate the advantages and importantly the efficiency of the approach chosen. Furthermore, important parameters such as the Sn metal loading and the influence of the electrolyte pH were investigated.

2 Experimental section

2.1 GDE preparation

The GDE was prepared using a newly developed dry pressing approach. The electrode comprises a mixture of acetylene black (Alfa-Aesar, 99.9 %), graphite (Timrex, T150), and PTFE (TF 9207Z, Dyneon) with a ratio of 4:1.5:3, and the active metal Sn (Sigma-Aldrich,

Fig. 1 Sketch of experimental set-up (RE = reference, W = working, C = counter electrode)



nanopowder, <150 nm, >99 % trace metals basis). The components were physically mixed in a knife mill (IKA M20 Universal mil) to obtain a homogeneous mixture, 750 mg was filled in a mask and pressed with a pressure of 11 kN cm^{-2} for 1 h on a 11.35 cm^2 hydrophobic gas diffusion layer (SGL, Sigracet GDL 35BC). The electrode obtained was sintered in an oven at $340 \text{ }^\circ\text{C}$, slightly above the melting point of PTFE for a period of 10 min in a nitrogen atmosphere.

2.2 Electrochemical reactor and experimental procedure

Experiments were conducted in a semi-batch cell schematically depicted in Fig. 1. It consists of a cathode and anode chamber which are separated by a proton conducting membrane (Nafion[®] 117, DuPont), so the produced formate can be accumulated on the cathode side, preventing it from being oxidized on the anode and to ensure the transport of cations from anode to the cathode. As counter electrode at the anode side, a Pt foil was utilized for the oxidation of water. The gas diffusion electrode (partially masked by plexiglas to obtain a geometric surface area of 1 cm^2) was used as cathode. CO_2 (Westfalen, 99.995 %) was continuously fed to the gas side at 3 mL min^{-1} , while the electrolyte was filled into cathode and anode chamber before the experiment. The cathode chamber was filled with 10 mL of 0.1 M aqueous KHCO_3 (Sigma-Aldrich, >99.99 % trace metal basis, water: Sigma-Aldrich, HPLC-grade) solution, the anode chamber with 18 mL 1 M KHCO_3 . The electrolyte was always pre-electrolyzed for 4 h at a voltage of 2 V to minimize contamination of the electrode surface by impurities and metal traces. For the experiments investigating the influence of the pH value, the

pH was adjusted by adding KOH solution (Sigma-Aldrich). Experiments were carried out at room temperature ($25 \pm 2.5 \text{ }^\circ\text{C}$) and ambient pressure and run for 1 h; Faradaic efficiencies are thus averaged over this time period. Current density was controlled and kept at a constant value with a potentiostat (Gamry, Reference3000), while the potential was evaluated over time. All potentials reported herein are potentials of the working electrode and compensated for the voltage drop in the electrolyte between working and reference electrode by the Gamry software via *iR*-drop measurements automatically conducted after each datapoint. As reference electrode, a Hg|HgO, 0.1 M KHCO_3 electrode was used ($E = 98 \text{ mV}$ vs. SHE at pH 14 and $25 \text{ }^\circ\text{C}$).

2.3 Analytics and characterization

The amount of formic acid produced was quantified using high pressure liquid chromatography with an Agilent Technology type 1200 equipped with a Nucleogel Sugar 810H column (Macherey–Nagel) and an RI detector. In order to evaluate gas phase composition online, gas chromatography was utilized on an Agilent Technologies 7890. Samples were injected through a HP-Plot Q (Agilent J&W) column equipped with an FID and through a Poropak Q and Molsieve 5A connected to the TCD. Combining both GC and HPLC, the current selectivity could be closed in between 5 % for all experiments. N_2 physisorption measurements were performed on an Autosorb-3B (Quantachrome) and evaluated by a multi-point method in the pressure range $p/p_0 = 0.05\text{--}0.3$ to obtain the BET surface area. The sample was outgassed at $110 \text{ }^\circ\text{C}$ for 16 h. In order to evaluate the dispersion of the catalyst, scanning electron microscopy (SEM) images have been taken at the

DLR with a Zeiss ULTRA plus microscope equipped with an AsB (angle selective backscattered electron) detector.

3 Results and discussion

3.1 GDE preparation and optimization

Since literature on the dry deposition of GDEs is relatively scarce [24, 26], an elaborate investigation and optimization was conducted in order to develop a simple, straightforward, and reproducible method for their preparation. The optimization of the composition (namely, the ratio of the components and type of carbon allotrope), the mixing, and the pressing procedure were conducted with the primary objective to obtain stable and reproducible electrodes with a maximum FE to CO₂ reduction. The exact preparation procedure is reported in the experimental section, while the approach is described in the following. As it was already suggested in literature, acetylene black exhibits very good performance characteristics as carbon substrate for GDEs because of its favorable channel network, pore distribution, and high electrical conductivity [27]. This is the case even though it exhibits a rather small surface area (BET: 75 m² g⁻¹) compared to other carbon materials such as activated carbon. The corresponding BET surface area of the GDEs prepared by the method reported herein was 16 m² g⁻¹ at a metal loading of 5 mg cm⁻². Problems arising in the ability to press the powder mixture onto the gas diffusion layer with satisfactory mechanical integrity were solved by the addition of graphite. The graphite with its soft texture decreases the brittleness of the pressed samples and makes them suitable for the experiments in the first place. As its addition further decreases the available surface area, it should not be employed at a ratio beyond what is necessary for successful pressing. The same accounts for PTFE as binding agent which is required to provide hydrophobicity to the pore system and to supply the matrix with stability by sticking the carbon and catalyst particles together. Just as for graphite, its amount was kept at a minimum to ensure these prerequisites without decreasing the performance of the GDE by making it too hydrophobic (impeding its wettability) and by the profuse blockage of diffusion channels. A concluding sintering step was added, at 340 °C slightly above the melting point of PTFE, as it further increases the stability of the GDE and allows for the deeper penetration of the PTFE into the pores. The development of this simple preparation procedure offers the opportunity for easy testing of GDEs with different compositions and their optimization. In this respect, the ratio of components that was determined to be the most suitable and thus employed in the following experiments constitutes as 4:1.5:3 with regard to acetylene

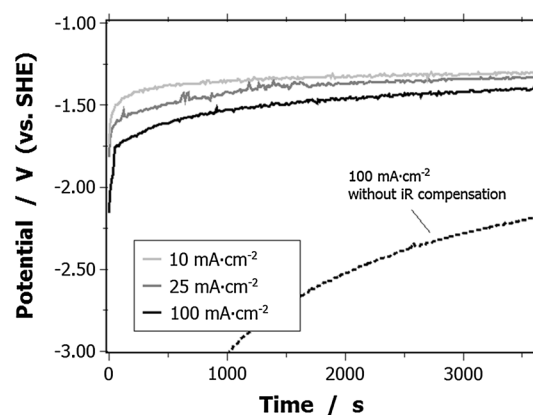


Fig. 2 Recorded iR-compensated cathode potential over time for different current densities and potential without iR compensation at 100 mA cm⁻² (dashed line), metal loading 5 mg cm⁻², pH 8.4

black, graphite, and PTFE. The investigation of the tin content is discussed below.

3.2 Electrochemical reduction

In the next sections, the performance of the prepared GDEs is evaluated. Therefore, galvanostatic semi-batch experiments were conducted as described in the experimental section. All the experiments reported have been reproduced at least twice to ensure that results were significant and not object to experimental deviations. The only products observed were formate, hydrogen, CO, and traces of methane. The sum of the corresponding FEs closed within 5 % at all times. Three such galvanostatic experiments are represented in Fig. 2 for current densities of 10 mA cm⁻², 25 mA cm⁻², and 100 mA cm⁻² at a pH value of 8.4 and a metal loading of 5 mg cm⁻². The current density was set to a fixed value and the resulting iR-compensated potential, i.e., the potential corrected for the ohmic drop in the electrolyte between working and reference electrode, was recorded over the course of each 1 h experiment. Additionally, the cathode potential *without* iR compensation for the 100 mA cm⁻² experiment is shown (dashed line) to provide information on its magnitude. As one can see, the difference between the two graphs, the iR compensation, decreases rapidly over time. This is due to the conductivity of the electrolyte increasing as formate is being accumulated. As a consequence, the ohmic drop also becomes smaller.

The first observation that the graph reveals is the time resolved behavior of the GDE potential which was consistently observed for all the experiments. After a short inductive period with a steep increase of the potential (getting less negative) linked to the polarization of the electrode, the rise of the potential slows down, yet still is

slightly and continuously increasing with time. This effect is more pronounced at higher current densities, thus, the potential difference for different current densities decreases over time. The fact that the GDE is indeed becoming increasingly active with time (less overpotential needed for the same current density) is a common phenomenon that has also been observed for GDEs in alkaline fuel cells. It can be attributed to changes in the hydrophobic network induced by the electrochemical stress and the resulting improvement of wettability of the electrodes by the electrolyte [28]. Yet, one should keep in mind that this can only proceed up to a certain point after which profuse flooding of the matrix occurs.

A problem which has been discussed in literature is the potential re-oxidation of formed formate at the anode. Although this can be mitigated by the use of a Nafion membrane separating anode and cathode space, it cannot be entirely prevented, as formate can still cross the membrane to the anode chamber in small amounts [29, 30]. This could give rise to incorrect results, especially at higher current densities and formate concentrations, thus, producing incorrect conclusions. However, if this was the case it would be noticed in the employed set-up as the sum of the FEs would no longer add up to 100 % because of the missing formate. In order to verify that this holds true, an experiment was conducted in which the reaction was started with a specified amount of formate already in the cathode chamber, and with nitrogen instead of CO₂ flowing on the gas side of the GDE. Accordingly, after the experiment no formate could be found on the anode side, while its concentration remained unchanged on the cathode side. This supports the above argument.

3.3 Effect of metal loading

Serving as the active component to promote the formation of formate and to suppress HER, Sn powder is added to the GDE mixture. Although the amount of metal used is a critical factor for the economic evaluation, only a few studies investigating the influence of metal loading on this reaction more extensively have been reported so far [8, 31]. In order to determine the optimum metal loading, and to elucidate its influence, GDEs with different amounts of metal ranging from 0 mg cm⁻² to 15 mg cm⁻² have been prepared, and their performance, i.e., the relationship between potential and current density, as well as the corresponding product specific FE, examined.

One important trend for increasing metal loadings is an increase in activity indicated by a higher current density at a given overpotential. This effect is shown in Fig. 3 for GDEs loaded with 1 mg cm⁻², 5 mg cm⁻², and 15 mg cm⁻² for which potentiodynamic scans have been conducted (scan rate 5 mV s⁻¹) after 1 h of reaction at

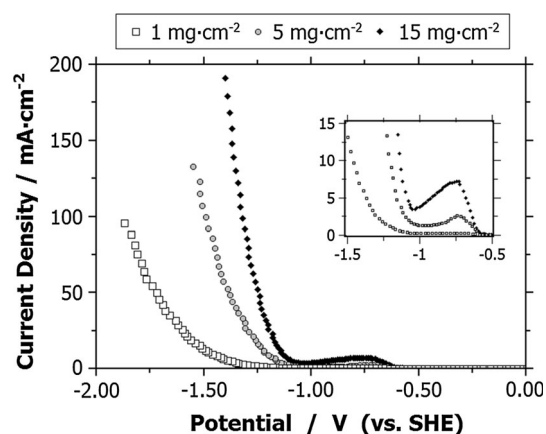


Fig. 3 Potentiodynamic Scan (5 mV s⁻¹) for GDEs with different Sn loading and magnification of Sn reduction peak, pH 10

50 mA cm⁻². Here, the current density is plotted over the iR-corrected potential. As can be seen, the onset of the reaction is approximately at the same potential (-1.0 V vs. SHE). However, at more negative potentials, the current density rises significantly faster for higher loadings, indicating that higher reaction rates can be achieved for the same applied reactor voltage. The small peak observed around -0.75 V can be attributed to the partial reduction of a thin tin oxide layer on the surface of the metal particles [32]. It is especially noticeable at higher loadings where more metal has to be reduced, see magnification.

The measurement of *total* current density alone does not give a sufficient assessment of the GDE performance as the *partial* current toward the desired product is in fact the crucial parameter. Hence, to calculate the respective FE the product distribution must be determined. Accordingly, the FE is depicted in Fig. 4 for an intermediate current density of 50 mA cm⁻² as a function of the metal loading. As can be seen, already in the absence of Sn, CO₂ reduction is observed with an FE of approximately 35 % toward formate and 2 % to CO, whereas the remainder accounts for HER. Electroreduction of CO₂ in the absence of metal catalyst has already been observed before [33, 34]. Due to the high overpotential toward the latter reaction, the addition of only small amounts of Sn substantially suppresses HER while CO₂ reduction is promoted. As can be seen, for a current density of 50 mA cm⁻² a loading as low as 0.2 mg cm⁻² was enough to increase the FE of formate to 93 %. It must be noted, however, that this minimum amount of metal depends on the desired productivity. For a current density of 200 mA cm⁻², e.g., and a loading of 0.2 mg cm⁻², the FE of hydrogen still accounts for 22 % (not shown here). At this current density, a loading of at least 1 mg cm⁻² was necessary to suppress HER below 3 %. At 50 mA cm⁻² and loadings up to 5 mg cm⁻², the

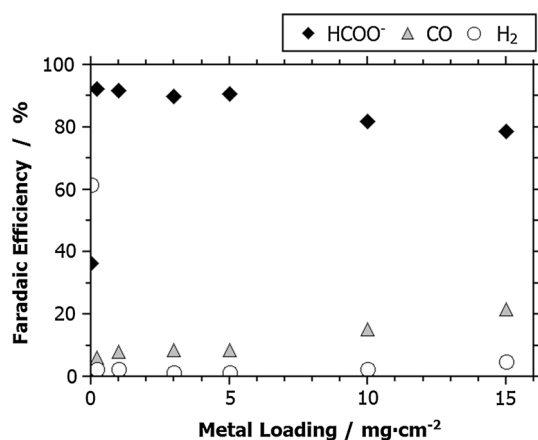


Fig. 4 Faradaic efficiency toward formate (black), CO (gray), and H₂ (white) as a function of the Sn metal loading at 50 mA cm⁻² and pH 10

FE for formate remained near 90 %, below 10 % for CO and 3 % for hydrogen. Beyond this loading, however, formate production was found to decline; to 82 % at 10 mg cm⁻² and 80 % at 15 mg cm⁻². The corresponding standard deviations for a loading of 5 mg cm⁻² are 1.02, 1.36, and 0.18 % for formate, CO, and H₂ FE, respectively (calculated for 6 GDEs). These small deviations in the results demonstrate both the reliable reproducibility of the preparation procedure but also that the decline in formate FE is significant, and not due to experimental uncertainties. Analysis of the product distribution shows that HER is still mostly suppressed, and that the decline of formate selectivity goes in favor of CO production which increases consistently.

It is suggested here that the shift in product distribution from formate to CO is attributed to the electrochemical characteristics of the electrode. As shown in Fig. 3, the metal loading has a significant influence on the resulting overpotential at a given current density. In the potentiodynamic experiment above for example, the difference at 50 mA cm⁻² between 1 mg cm⁻² and 15 mg cm⁻² is as high as 0.4 V (-1.3 V / -1.7 V vs. SHE). Conversely, the reaction rates for different reactions (here: CO vs. formate vs. hydrogen production) are influenced by the potential to various degrees which results in the known fact that different product distributions are obtained depending on the applied potential. In literature, it has been shown that for different formate producing catalysts, at moderate and high overpotentials formate dominates over CO production. However, going to lower overpotentials the FE toward CO increases [13, 35] as it is observed here when higher metal loadings are employed. The same trend can also be seen for experiments at low current density which are described below (see Fig. 5). Thus, the fact that higher loadings result

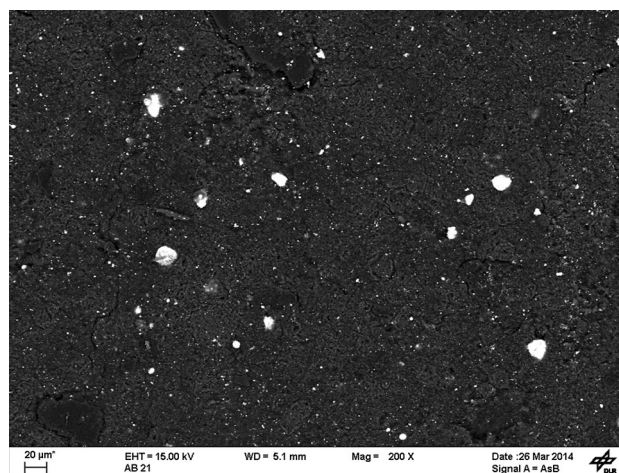


Fig. 5 SEM image of GDE (5 mg cm⁻²) taken with an AsB detector to visualize tin dispersion (white color), bar says 20 μm, beam energy 15 kV, magnification 200x

in a lower cathode potential can explain the shift toward CO production. Finally, also the results for subsequent experiments performed on one GDE and even consecutive GC measurements during one experiment are consistent with this explanation: as the cathode potential constantly decreases with time, the product distribution of CO₂ reduction slightly but steadily shifts toward CO in the same manner. This fact might constitute a severe challenge that must be approached in further studies of the GDE performance that will be performed in the near future.

Another point that needs to be addressed regarding the metal loading is the utilization of the catalyst and the metal dispersion. Fig. 5 shows an SEM image of the GDE after sintering. Using an AsB (angle selective backscattered electron) detector allows one to distinguish between the components on the image of a sample as heavier elements appear brighter, in this case the tin particles. As one might already expect, due to the way the catalyst is introduced into the GDE, and the fact that the sintering temperature is above the melting point of tin (340 °C vs. 232 °C), the images show that the catalyst distribution is very non-uniform and the nanoparticles agglomerate to particles up to several μm. In contrast, a very high dispersion is aimed for as one wants to minimize the amount of metal catalyst. This cannot be achieved with the current method and leaves room for improvement. However, even though this is the case, the GDE gives very promising results also at low loadings that are typical for GDEs. Supporting the nanoparticles on the carbon black before pressing the GDE could be a practical way to ensure a high dispersion and to increase the utilization of the catalyst, an approach which will be investigated in the near future.

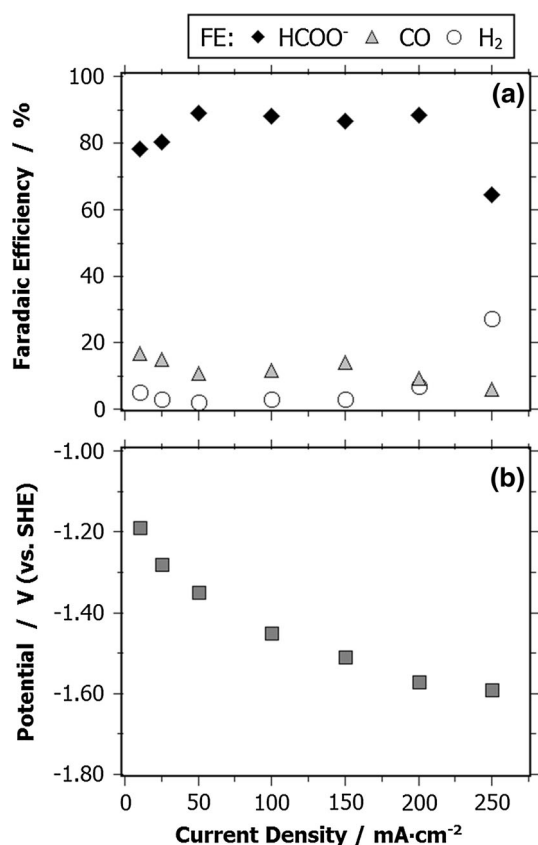


Fig. 6 Faradaic efficiencies for HCOO⁻, CO, and H₂ (a) and potential (b) as a function of current density, at metal loading of 5 mg cm⁻² and pH 8.4

The above results show an “optimum” metal loading depends on several parameters, in the end constituting a compromise that must be assessed by an economic evaluation. For monetary reasons, the mass of metal should be kept at a minimum, whereas low loadings come with the drawback of low electrode activity and require higher overpotentials for a given conversion. Furthermore, its influence on the product distribution is of crucial importance. In this respect, when a loading above 5 mg cm⁻² is to be employed, the benefit of low overpotentials is overcome by the problem that the FE increasingly shifts from formate to CO production at a given current density. Therefore, as a trade-off a loading of 5 mg cm⁻² has been chosen in the following for further investigation.

3.4 Current density, applied potential, and faradaic efficiency

An important characteristic of an electrochemical system is the relationship between potential, the resulting current density, and the corresponding FE. Because the advantage of GDEs is their ability to overcome mass transport limitations, the current density up to which the system can

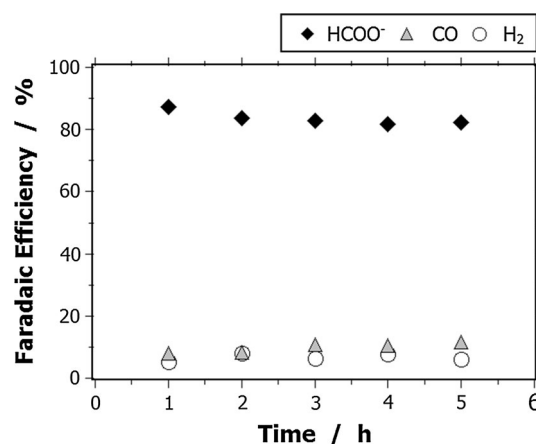


Fig. 7 Faradaic efficiencies for HCOO⁻, CO, and H₂ for consecutive experiments using the same GDE (5 mg cm⁻²) at 200 mA cm⁻² and pH 10

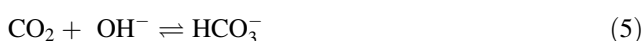
operate without a substantial loss of FE is of particular interest. All of these parameters can be extracted from Fig. 6a, b. The cathode potentials that correspond to the specific current densities are taken from the potentiodynamic scan described earlier. As can be seen in Fig. 6a, the product distribution for 50 mA cm⁻² can be maintained very constantly also at higher current density up to 200 mA cm⁻². Only above this value mass transport limitations do become an issue, resulting in an increase of HER to about 27 % at 250 mA cm⁻². At this current density, the reaction rate becomes so high that the diffusion of the reactants to the active site cannot keep up anymore and hydrogen production proceeds instead. On the other hand, at low potentials and current densities a slight decrease of formate production in favor of CO is evident (79 % formate, 17 % CO at 10 mA cm⁻²); HER also slightly increases. This is in accordance with the observation above which suggested that CO production is favored on GDEs with high loadings because of their low cathode potentials. Indeed, the corresponding potential of -1.28 V at 25 mA cm⁻² is very close to the above -1.30 V at 50 mA cm⁻² and 15 mg cm⁻² loading, both resulting in an FE of around 80 %. These results are very promising as a current density as high as 200 mA cm⁻² and 90 % FE at the same time has not yet been reported for the production of formate at ambient pressure. The corresponding cathode potential was measured to be 1.57 V vs. SHE what is in the range of what has been reported before.

Although the stability over a longer period of time is a basic requirement of any application and has to be evaluated at some point, the actual long-term behavior of the GDE performance is not subject of this study. However, in order to show that the electrode does not exhibit fast initial deactivation, and that one can maintain the yield of formate

for a few hours, consecutive experiments have been conducted using the same GDE at 200 mA cm^{-2} and pH 10. In between these experiments, the electrolyte has been changed and the reactor rinsed with distilled water. The FE over the course of these experiments is shown in Fig. 7. One can clearly see that the reaction can be operated with a relatively stable performance over at least 5 h. The FE toward formate stays nearly constant and only slightly decreases from 87 to 82 % in this time period. As mentioned above, this shift of product distribution over time goes in favor of CO production and not HER. Even though this is already a promising result, long-term stability still has to be demonstrated, as done for example in [36, 37].

3.5 Effect of pH value on product distribution

The choice of the electrolyte is a crucial parameter in the reduction of CO_2 that has been investigated extensively [25, 41]. While ambiguity exists, KHCO_3 has been suggested by several authors to be advantageous due to its ability to buffer the pH near the cathode surface and the effect it has on production rate and FE [18, 38]. Thus, KHCO_3 was chosen as electrolyte in this study. In addition to the identity of the electrolyte, it has been sufficiently demonstrated that its pH value has a substantial effect on the product distribution which varies according to the electrolyte used and the system studied [18, 25, 39]. However, the conclusions from literature on the choice of the optimum pH differ and even contradict each other to a certain degree. In basic aqueous media dissolved CO_2 is converted into the $\text{HCO}_3^-/\text{CO}_3^{2-}$ equilibrium according to Eq. 5. These species are considered to be inactive or at least not active to a significant degree for CO_2 reduction [4].



This seems to suggest that CO_2 reduction should be conducted in acidic to neutral solution, where the electrochemically active species $\text{CO}_{2,\text{aq}}$ prevails. Yet, the pH also influences the competing HER, as its potential in acidic to neutral media is proportional to proton activity [40]. Accordingly, at low pH HER is suggested to dominate over CO_2 reduction [41]. Due to the complex interaction of the above influences, especially when a buffer solution such as KHCO_3 is employed, there is an obvious difficulty in predicting the ideal pH concerning productivity. Therefore, the effect of pH on the product distribution was examined as part of this study. This was done in order to determine if the GDE performance can be further improved by the adjustment of the pH, and to see how robust the system is toward pH gradients. These gradients are often problematic in applications where they commonly occur over the length of the electrochemical reactor due to accumulation of

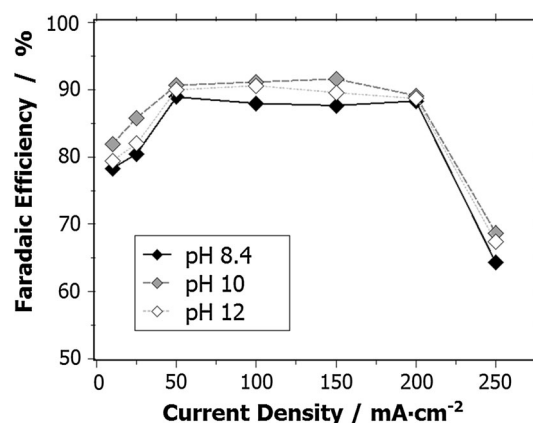


Fig. 8 Faradaic efficiency as a function of the applied current density for different pH values, metal loading 5 mg cm^{-2}

products. It should be noted here that during the reaction the local pH near the surface may deviate substantially from that of the bulk, as studied by Gupta et al. [42]. However, the scope of this study was not to elucidate pH influences for mechanistic aspects but rather to evaluate the formerly mentioned points.

The pH was adjusted with KOH between 8.4 and 12 and the FE evaluated for different current densities. The obtained results are depicted in Fig. 8. The results show that the product distribution is not as significantly affected by the pH value in the system at hand as it was in other studies. Only a very slight trend is noticeable that suggests the FE undergoes a small optimum at a pH value of 10, especially noticeable in the low current density region. Since all the experiments have been conducted at least twice and the results averaged, this finding cannot be attributed to experimental uncertainties alone, keeping in mind the low standard deviation reported above. It supports the above argument that the choice of the pH marks a compromise between the different factors governing the pH influence, and must be evaluated for each system separately. Conversely, the reason why this influence was almost negligible here can be explained by the fact that HER, the reaction on which the pH has an effect on, was almost entirely suppressed to very low values and has therefore no significant influence on the overall product distribution. Furthermore, compared to conventional electrolysis, CO_2 in a GDE is fed in the gas phase from which it directly diffuses to the three-phase boundary where it is being converted. Thus, it only diffuses rather small distances into the electrolyte, and is not substantially impaired by the OH^- concentration, as it would be the case in CO_2 -saturated electrolyte where the pH determines the amount of electro-active species. This holds especially true since conversion with OH^- (Eq. 5) is known to happen at rather

slow rate [4]. Finally, it must be kept in mind, as mentioned above, that the pH near the cathode surface can strongly deviate from the bulk and also from the starting pH, because of the products produced and the buffer solution employed. This means that for the experiments the difference in the actual pH at the cathode surface during the electrolysis can be much different to the difference of the starting pH (e.g. 8.4 vs. 12).

Nevertheless, this insensitivity of the system toward pH gradients is of great interest for technical application since local pH gradients in electrochemical reactors are a common problem for electrochemical processes that might occur due to product accumulation over the length of the reactor.

4 Conclusion

The work presented in this study has demonstrated the development of the preparation procedure of GDE from a powder mixture of Sn, acetylene black, graphite, and PTFE via a dry deposition method. This procedure comes with the advantage of preparing GDEs with a high reproducibility in a very easy, fast, and straightforward manner without the use of any solvent. In this respect, also the influence of the metal loading has been investigated. It has been shown that the amount of metal has not only an influence on the necessary overpotential for a given current density but also on the product distribution. This is due to the effect the amount of metal has on the necessary overpotential of the reaction. A low metal loading gives high FE toward formate (up to 93 % at 50 mA cm⁻²) but introduces the drawback of higher reactor voltage for a given current density. Conversely, at high metal loading lower reactor voltages can be obtained at the same current density but as a result the product distribution shifts from formate to CO. The minimum loading to substantially suppress HER at the highest current density of 200 mA cm⁻² was 1 mg cm⁻² of Sn. Furthermore, the influence of the starting pH value of the electrolyte has been examined in the basic regime using KHCO₃ as the electrolyte. The results suggest that this system is relatively insensitive to pH gradients but still shows a slight maximum for formate FE at pH 10. At this value, the GDE utilization allows for the production of formate at current densities up to 200 mA cm⁻² with a FE of around 90 %, the rest accounting for CO (≈ 8 %) and H₂ at a loading of 5 mg cm⁻². The obtained results herein are promising as such a high current density toward formate combined with the simultaneous suppression of HER at ambient pressure has not yet been reported. The corresponding iR-compensated cathode potential was at 1.57 V vs. SHE. Although these results are very promising, they can only serve as

basis for further investigation. Importantly, further work must investigate the feasibility of transferring this approach from semi-batch mode to continuous mode of operation and evaluate the long-term stability of the GDE performance.

Acknowledgments The authors would like to thank the German BMWi (Bundesministerium für Wirtschaft und Energie) for the financial support (03ET1037B), Ina Plock (DLR) for taking SEM images, Alexander Bauder (DLR) and the project partners (DLR, INVENIOS Europe GmbH, Plinke GmbH) for their collaboration. Special thanks also go to Prof. Albert Renken, EPFL Lausanne, for the fruitful discussions.

References

1. Aresta M, Dibenedetto A (2007) Utilisation of CO₂ as a chemical feedstock: opportunities and challenges. *Dalton Trans* 28:2975–2992. doi:10.1039/b700658f
2. Hu B, Guild C, Suib SL (2013) Thermal, electrochemical, and photochemical conversion of CO₂ to fuels and value-added products. *J CO₂ Util* 1:18–27. doi:10.1016/j.jcou.2013.03.004
3. Ausfelder F, Bazzanella A (2008) Dechema Diskussionspapier: Verwertung und Speicherung von CO₂. Dechema e.V.
4. Hori Y (2008) Electrochemical CO₂ reduction on metal electrodes. *Mod Asp Electrochem* 42:89–189. doi:10.1007/978-0-387-49489-0_3
5. Scibioh M, Viswanathan B (2004) Electrochemical reduction of carbon dioxide: a status report. *Proc Indian Natl Sci Acad* 70:407–462
6. Whipple DT, Kenis PJA (2010) Prospects of CO₂ utilization via direct heterogeneous electrochemical reduction. *J Phys Chem Lett* 1:3451–3458. doi:10.1021/jz1012627
7. Oloman C, Li H (2008) Electrochemical processing of carbon dioxide. *ChemSusChem* 1:385–391. doi:10.1002/cssc.200800015
8. Ma S, Lan Y, Perez GMJ, Moniri S, Kenis PJA (2014) Silver supported on titania as an active catalyst for electrochemical carbon dioxide reduction. *ChemSusChem* 7:866–874. doi:10.1002/cssc.201300934
9. Dufek EJ, Lister TE, McIlwain ME (2011) Bench-scale electrochemical system for generation of CO and syn-gas. *J Appl Electrochem* 41:623–631. doi:10.1007/s10800-011-0271-6
10. Alvarez-Guerra M, Quintanilla S, Irabien A (2012) Conversion of carbon dioxide into formate using a continuous electrochemical reduction process in a lead cathode. *Chem Eng J* 207–208:278–284. doi:10.1016/j.cej.2012.06.099
11. Prakash GS, Viva FA, Olah GA (2013) Electrochemical reduction of CO₂ over Sn-Nafion[®] coated electrode for a fuel-cell-like device. *J Power Sources* 223:68–73. doi:10.1016/j.jpowsour.2012.09.036
12. Loges B, Boddien A, Gärtner F, Junge H, Beller M (2010) Catalytic generation of hydrogen from formic acid and its derivatives: useful hydrogen storage materials. *Top Catal* 53:902–914. doi:10.1007/s11244-010-9522-8
13. Makowski P, Thomas A, Kuhn P, Goettmann F (2009) Organic materials for hydrogen storage applications: from physisorption on organic solids to chemisorption in organic molecules. *Energy Environ Sci* 2:480–490. doi:10.1039/b822279g
14. Azuma M (1990) Electrochemical reduction of carbon dioxide on various metal electrodes in low-temperature aqueous KHCO₃ media. *J Electrochem Soc* 137:1772–1776. doi:10.1149/1.2086796
15. Hori Y, Wakebe H, Tsukamoto T, Koga O (1994) Electrocatalytic process of CO selectivity in electrochemical reduction of

- CO₂ at metal electrodes in aqueous media. *Electrochim Acta* 39:1833–1839. doi:10.1016/0013-4686(94)85172-7
16. Noda H, Ikeda S, Oda Y, Imai K, Maeda M, Ito K (1990) Electrochemical reduction of carbon dioxide at various metal electrodes in aqueous potassium hydrogen carbonate solution. *Bull Chem Soc Jpn* 63:2459–2462. doi:10.1246/bcsj.63.2459
 17. Mahmood MN, Masheder D, Harty CJ (1987) Use of gas-diffusion electrodes for high-rate electrochemical reduction of carbon dioxide. I. Reduction at lead, indium- and tin-impregnated electrodes. *J Appl Electrochem* 17:1159–1170. doi:10.1007/BF01023599
 18. Whipple DT, Finke EC, Kenis PJA (2010) Microfluidic reactor for the electrochemical reduction of carbon dioxide: the effect of pH. *Electrochem Solid-State Lett* 13:B109–B111. doi:10.1149/1.3456590
 19. Furuya N, Yamazaki T, Shibata M (1997) High performance Ru-Pd catalysts for CO₂ reduction at gas-diffusion electrodes. *J Electroanal Chem* 431:39–41. doi:10.1016/S0022-0728(97)00159-9
 20. Hara K (1997) Electrocatalytic formation of CH₄ from CO₂ on a Pt gas diffusion electrode. *J Electrochem Soc* 144:539–545. doi:10.1149/1.1837445
 21. Cook RL (1990) High rate gas phase CO₂ reduction to ethylene and methane using gas diffusion electrodes. *J Electrochem Soc* 137:607–608. doi:10.1149/1.2086515
 22. Dufek EJ, Lister TE, Stone SG, McIlwain ME (2012) Operation of a pressurized system for continuous reduction of CO₂. *J Electrochem Soc* 159:F514–F517. doi:10.1149/2.011209jes
 23. Gülzow E, Schulze M, Wagner N, Kaz T, Reissner R, Steinhilber G, Schneider A (2000) Dry layer preparation and characterisation of polymer electrolyte fuel cell components. *J Power Sources* 86:352–362. doi:10.1016/S0378-7753(99)00451-6
 24. Yu J, Yoshikawa Y, Matsuura T, Islam MN, Hori M (2005) Preparing gas-diffusion layers of PEMFCs with a dry deposition technique. *Electrochem Solid-State Lett* 8:A152–A155. doi:10.1149/1.1854119
 25. Li H, Oloman C (2006) Development of a continuous reactor for the electro-reduction of carbon dioxide to formate—Part 1: process variables. *J Appl Electrochem* 36:1105–1115. doi:10.1007/s10800-006-9194-z
 26. Wagner N (2004). Verfahren und Vorrichtung zur Herstellung einer Elektrode. Patent No. DE 19940015 B9. Germany
 27. Park S, Lee J, Popov BN (2012) A review of gas diffusion layer in PEM fuel cells: materials and designs. *Int J Hydrog Energy* 37:5850–5865. doi:10.1016/j.ijhydene.2011.12.148
 28. Wagner N, Schulze M, Gülzow E (2004) Long term investigations of silver cathodes for alkaline fuel cells. *J Power Sources* 127:264–272. doi:10.1016/j.jpowsour.2003.09.022
 29. Lv W, Zhang R, Gao P, Lei L (2014) Studies on the faradaic efficiency for electrochemical reduction of carbon dioxide to formate on tin electrode. *J Power Sources* 253:276–281. doi:10.1016/j.jpowsour.2013.12.063
 30. Li H, Oloman C (2007) Development of a continuous reactor for the electro-reduction of carbon dioxide to formate—Part 2: scale-up. *J Appl Electrochem* 37:1107–1117. doi:10.1007/s10800-007-9371-8
 31. Wu J, Sharma PP, Harris BH, Zhou X (2014) Electrochemical reduction of carbon dioxide: IV dependence of the Faradaic efficiency and current density on the microstructure and thickness of tin electrode. *J Power Sources* 258:189–194. doi:10.1016/j.jpowsour.2014.02.014
 32. Zhang S, Kang P, Meyer TJ (2014) Nanostructured tin catalysts for selective electrochemical reduction of carbon dioxide to formate. *J Am Chem Soc* 136:1734–1737. doi:10.1021/ja4113885
 33. Zhang S, Kang P, Ubnoske S, Brenneman MK, Song N, House RL, Glass JT, Meyer TJ (2014) Polyethylenimine-enhanced electrocatalytic reduction of CO₂ to formate at nitrogen-doped carbon nanomaterials. *J Am Chem Soc* 136:7845–7848. doi:10.1021/ja5031529
 34. Hara K, Kudo A, Sakata T (1995) Electrochemical reduction of carbon dioxide under high pressure on various electrodes in an aqueous electrolyte. *J Electroanal Chem* 391:141–147. doi:10.1016/0022-0728(95)03935-A
 35. Todoroki M, Hara K, Kudo A, Sakata T (1995) Electrochemical reduction of high pressure CO₂ at Pb, Hg and In electrodes in an aqueous KHCO₃ solution. *J Electroanal Chem* 394:199–203. doi:10.1016/0022-0728(95)04010-L
 36. Agarwal AS, Zhai Y, Hill D, Sridhar N (2011) The electrochemical reduction of carbon dioxide to formate/formic acid: engineering and economic feasibility. *ChemSusChem* 4:1301–1310. doi:10.1016/0022-0728(95)03935-A
 37. Chen Y, Li CW, Kanan MW (2012) Aqueous CO₂ reduction at very low overpotential on oxide-derived Au nanoparticles. *J Am Chem Soc* 134:19969–19972. doi:10.1021/ja309317u
 38. Wu J, Risalvato FG, Ke F, Pellechia PJ, Zhou X (2012) Electrochemical reduction of carbon dioxide I. Effects of the electrolyte on the selectivity and activity with Sn electrode. *J Electrochem Soc* 159:F353–F359. doi:10.1149/2.049207jes
 39. Innocent B, Liaigre D, Pasquier D, Ropital F, Léger J, Kokoh KB (2009) Electro-reduction of carbon dioxide to formate on lead electrode in aqueous medium. *J Appl Electrochem* 39:227–232. doi:10.1007/s10800-008-9658-4
 40. Gattrell M, Gupta N, Co A (2006) A review of the aqueous electrochemical reduction of CO₂ to hydrocarbons at copper. *J Electroanal Chem* 594:1–19. doi:10.1016/j.jelechem.2006.05.013
 41. Hori Y, Suzuki S (1982) Electrolytic reduction of carbon dioxide at mercury electrode in aqueous solution. *Bull Chem Soc Jpn* 55:660–665. doi:10.1246/bcsj.55.660
 42. Gupta N, Gattrell M, MacDougall B (2006) Calculation for the cathode surface concentrations in the electrochemical reduction of CO₂ in KHCO₃ solutions. *J Appl Electrochem* 36:161–172. doi:10.1007/s10800-005-9058-y